Int. J. Nonlinear Anal. Appl. 12 (2021) No. 2, 2359-2372
ISSN: 2008-6822 (electronic)
http://dx.doi.org/10.22075/ijnaa.2021.5382

Inclined magnetic field and heat transfer of asymmetric and Porous Medium Channel on hyperbolic tangent peristaltic flow

Shahad Ali Abdulla[a,*], Liqaa Zeki Hummady[a]

[a]Department of Mathematic, University of Baghdad, Baghdad, Iraq

(Communicated by Madjid Eshaghi Gordji)

Abstract

The present study deal with the effective heat transfer with the activity of connected inclined magnetic field of the asymmetric channel through the porous medium. The effect of sliding speed on channel walls was taken into account and the effect of nonlinear particle size was analyzed applying long wavelength and low Reynolds count estimates. The mathematical expression of axial velocity, stream function and pressure rise was analytically determined. The effect of the physical parameter is included in the present model on the computational results. They are presented in chart form by applying for the Mathematica program.

Keywords: Inclined magnetic flied, Hyperbolic tangent, heat transfer and peristaltic flow

1. Introduction

The phenomenon of periscope carriage is a form of stuff carriage that Engenders in progressive wave unclasping or systole which is deploy along the length of a distensible tube.the topic of periscope is fountains consequential in chatted applied mathematics geometry and physiological world this is because of its many applications in genuine life example blood pumping machines biomedical geometry cancers therapy geophysics and many others the vital studies in this articulated are [3] act regarding peristaltic flow below the effect of paramagnetic field and hotness convection in different situations consulted by studies [11, 4] sundry instances other hand flow through porous medium have Numerous Applicative applications such as bio mechanics Fabrication candidacy of fiuids in the

*Corresponding author
Email addresses: ggha79391@gmail.com (Shahad Ali Abdulla), liqaa.hummady@sc.uobaghdad.edu.iq (Liqaa Zeki Hummady)

Received: March 2021 *Accepted:* July 2021

chatted fabricating human lung in the gall bladdre with emeris in small blood ships these a chieved the the peristaltic conveyed in an symmetric channel and the effect of careened paramagnetic field on magneto fluid flow through porous medium [2, 1] debated , the impact of MHD peristaltic conveyance throught poros medium stumble conditions play an indis pensable turn in turn in many applications rather than the no-slip conditions like. (Polymer ,industry) engineering medical application(polishing artificial heart) and technoiogcal, process may reserarches have been made on the slip condtion and its impacts ,on peristaltic flow of non-Now tonian fluids sevral non-Newtoian fluids such as polymer Ablates blood and multing rade oil can be bis criminate its according to own lmmanent equation the relation between shear stress and the rate of deformation [8] Among several non-Newtoninal fluid hyperbolic tangent model is one of the non-Newtoian models [10] foreword an betail study On the peristaltic conreyance of a hyperbolic tangent fluid in an asymmetric channel [9] lately studies the influence of an in inclined faramagntic field on peristaltic commuter ofa hyperbolic tangent nonoflliud inan inclined Aqueduct having flexile walls the target of the preset attain is to study the lmpact of inclined paramagnetic field on the peristaltic commuter of non-Newtoninan fluid in anti-symmetric porous Aqueduct the non-Newtonian fluid is hyperblic tangent fluid model the attain is done by applying the assumption of lengthy wavelengnth and low Reynolds number [5] the non-linear. Thethermodynamicfa parts of blood mayesy not be indispensable when the blood is inside the body yet it winds up basic when it is pulled out of the body. Considering the hugeness of heat transfer in circulation system [6] analyzed the thermodynamic pieces of circulatory system in the blood-viewing tube as the Cassone liquid. [7] Examination of warmth temperature to the springflow of fluid Directed through a penetrable redirect inside seeing the MHD. An activity on the trading of solids to the weight fluid by techniques for a disproportionate and non uniform channel in a porous medium. Adjudge equations were unlaced using regular perturbation technical for asmall weissenberg number for the stream function and the velocity are Accessing and the results were analyzed and shown graphically.

2. Mathematical Formulation

Consider the two dimensional flow of incompressible hyperbolic tangent fluid in an asymmetric channel having width $d_1 + d_2$. The flow is caused by infinite sinusoidal wave train moving ahead with constant velocity c along the walls of the channel. Different wave amplitudes, phase angle and channel widths result in an asymmetric channel. The geometries of the walls are modeled as

$$\begin{aligned} \bar{h}_1(\bar{x}, \bar{t}) &= d_1 + a_1 \sin\left(\frac{2\pi}{\lambda}(\bar{x} - c\bar{t})\right) \qquad \text{upper wall} \\ \bar{h}_2(\bar{x}, \bar{t}) &= d_2 + a_2 \sin\left(\frac{2\pi}{\lambda}(\bar{x} - c\bar{t}) + \phi\right) \qquad \text{lower wall,} \end{aligned} \tag{2.1}$$

where $a_1, a_2, d_1, d_2, \lambda, c, t$ are the amplitudes of the waves , ,width of the channel ,wavelength, wave speed $\phi, (0 \leq \phi \leq \pi)$ the phase difference and the rectangular coordinate system is chosen in such a way that X -axis lies in the direction of wave propagation and Y -axis perpendicular to X . It is noticed that $\phi = 0$ corresponds to symmetric channel with waves out of phase and for $\phi = \pi$ the waves are in phase. Further, a_1, a_2, d_1, d_2 and ϕ satisfy the condition $a_1^2 + a_2^2 + 2a_1a_2\cos(\phi) \leq (d_1 + d_2)^2$. The constitutive equation forhyperbolic tangent fluid (following Pop and Ingham is given by

$$\tau = -\Big(\eta_\infty + (\eta_0 + \eta_\infty)\tanh(\Gamma_\gamma)^n\Big)\gamma \tag{2.2}$$

η_∞ is the infant shear rate viscosity, η_0 is the zero shear rate viscosity, Γis the time constant, n is the power-law index and $\dot{\gamma}$is defined as

$$\dot{\gamma} = \sqrt{\frac{1}{2}\sum_i \sum_j \dot{\gamma}_{\text{ij}}\ \dot{\gamma}_{\text{ji}}} = \sqrt{\frac{1}{2}} \tag{2.3}$$

Here is the second invariant strain tensor. We consider the consititutive equation ( ), the case for which η_∞=0 and $\Gamma\dot{\gamma} < 1$. The component of extra stress tensor can be written as

$$\begin{aligned} \tau &= -\left[(\eta_0(\Gamma\dot{\gamma})^n\right]\dot{\gamma} \\ \tau &= -\left[(\eta_0(1 + n(\Gamma\dot{\gamma} - 1)\right]\dot{\gamma} \end{aligned} \tag{2.4}$$

It is further assumed that there is no motion of walls in the longitudinal direction. This assumption restrict the deformation of the walls , it does not imply that the channel is rigid along the longitudinal motions.

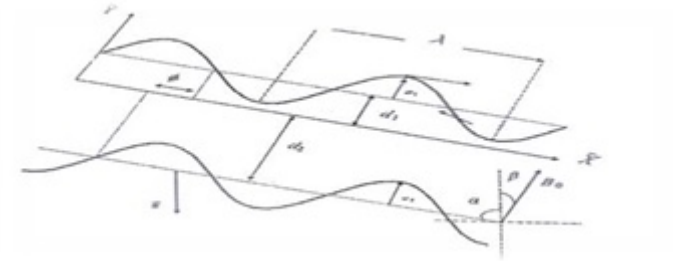

Figure 1: A physical sketch of the problem

3. Governing Equation

The governing equations of the motion in an inclined channel and inclined magnetic field of hyperbolic tangent fluid in the laboratory frame $(\bar{x}, \bar{y})$ can be written as

$$\frac{\partial \bar{u}}{\partial \bar{x}} + \frac{\partial \bar{v}}{\partial \bar{y}} = 0 \tag{3.1}$$

$$\rho(\frac{\partial}{\partial \bar{t}} + \bar{u}\frac{\partial}{\partial \bar{x}} + \bar{v}\frac{\partial}{\partial \bar{y}})\bar{u} = -\frac{\partial \bar{p}}{\partial \bar{x}} + \frac{\partial}{\partial \bar{x}}\bar{\tau}_{\bar{x}\bar{x}} + \frac{\partial}{\partial \bar{y}}\bar{\tau}_{\bar{x}\bar{y}} - \sigma B_0^2 \cos\beta^*(\bar{u}\cos\beta^* - \bar{v}\sin\beta^*) - \eta_0\frac{\bar{u}}{\bar{k}} \tag{3.2}$$

$$\rho(\frac{\partial}{\partial \bar{t}} + \bar{u}\frac{\partial}{\partial \bar{x}} + \bar{v}\frac{\partial}{\partial \bar{y}})\bar{v} = -\frac{\partial \bar{p}}{\partial \bar{y}} + \frac{\partial}{\partial \bar{x}}\bar{\tau}_{\bar{x}\bar{y}} + \frac{\partial}{\partial \bar{y}}\bar{\tau}_{\bar{y}\bar{y}} + \sigma B_0^2 \sin\beta^*(\bar{u}\cos\beta^* - \bar{v}\sin\beta^*) - \eta_0\frac{\bar{v}}{\bar{k}} \tag{3.3}$$

$$\rho C_p(\frac{\partial}{\partial \bar{t}} + \bar{u}\frac{\partial}{\partial \bar{x}} + \bar{v}\frac{\partial}{\partial \bar{y}})\bar{T} = k'(\frac{\partial^2}{\partial \bar{t}^2} + \frac{\partial^2}{\partial \bar{x}^2} + \frac{\partial^2}{\partial \bar{y}^2})\bar{T} + \eta_0[(\frac{\partial \bar{u}}{\partial \bar{x}} + \frac{\partial \bar{v}}{\partial \bar{y}})^2 + 2(\frac{\partial^2 \bar{u}}{\partial x^2})^2 + 2(\frac{\partial^2 \bar{v}}{\partial y^2})] \tag{3.4}$$

where the$\rho, \bar{u}, \bar{v}, \bar{y}, \bar{p}, \eta_0, k_0, \bar{k}, B_0, \sigma$ are the fluid density ,axial velocity , transverse velocity, transverse coordinate , pressure, viscosity , material constant, permeability parameter, constant magnetic field, is the electrical conductivity. The flow is unsteady in the laboratory frame $(\bar{x}, \bar{y})$. However in a coordinate system moving with the wave speed c (in wave frame $(\bar{X}, \bar{Y})$,the motion is steady. The following expressions

$$\bar{X} = \bar{x} - c\bar{t},\ \ \bar{Y} = \bar{y},\ \ \bar{U} = \bar{u} - c,\ \ \bar{V} = \bar{v},\ \ \bar{P}(\bar{X}, \bar{Y}) = \bar{P}(\bar{x}, \bar{y}, \bar{t}) \tag{3.5}$$

where $\bar{U}, \bar{V}, \bar{P}$ represent the velocity components and pressure in the wave frame.

To carry out the non-dimensional analysis we set up the following non-dimensional quantities

$$x = \frac{\bar{x}}{\lambda},\ \ y = \frac{\bar{y}}{d_1},\ \ u = \frac{\bar{u}}{c},\ \ v = \frac{\bar{v}}{c}, h_1 = \frac{\bar{h_1}}{d_1},\ \ h_2 = \frac{\bar{h_2}}{d_1},\ \ p = \frac{\bar{p}d_1^2}{\eta_0 c\lambda}, Da = \frac{\bar{k}}{d_1^2},\ \ Re = \frac{\rho c d_1}{\eta_0},$$
$$\delta = \frac{d_1}{\lambda},\ \ Ha = d_1\sqrt{\frac{\sigma}{\eta_0}}B_0,\ \ \tau = \frac{d_1}{\eta_0 c}\bar{\tau},\ \ We = \frac{\Gamma c}{d_1}, t = \frac{c\bar{t}}{\lambda}, \theta = \frac{(\bar{T}-\bar{T}_0)}{(\bar{T}_1-\bar{T}_0)},\ \ Ec = \frac{c^2}{c_p(\bar{T}-\bar{T}_0)}, \tag{3.6}$$
$$p_r = \frac{\mu c_p}{k}$$

where (δ) is the wave number, (Re) is the Renold number, (We) is the Weissenberg number, (Ha) is the Hartman number,

(We) Then, in view of Eq (2), Eqs. (3) to (4) take the form

$$\delta\frac{\partial u}{\partial x} + \frac{\partial v}{\partial y} = 0 \tag{3.7}$$

$$Re(\delta\frac{\partial u}{\partial t} + \delta u\frac{\partial u}{\partial x} + v\frac{\partial u}{\partial y}) = -\frac{\partial p}{\partial x} + \delta\frac{\partial \tau_{xx}}{\partial x} + \frac{\partial \tau_{xy}}{\partial y} - Ha^2\cos\beta^*(u\cos\beta^* - v\sin\beta^*) - \frac{u}{\mathrm{Da}} \tag{3.8}$$

$$Re\delta(\delta\frac{\partial v}{\partial t} + \delta u\frac{\partial v}{\partial x} + v\frac{\partial v}{\partial y}) = -\frac{\partial p}{\partial y} + \delta^2\frac{\partial \tau_{xy}}{\partial x} + \delta\frac{\partial \tau_{yy}}{\partial y} + Ha^2\delta\sin\beta^*(u\cos\beta^* - v\sin\beta^*) - \delta\frac{v}{\mathrm{Da}} \tag{3.9}$$

$$Re\sigma(\frac{\partial}{\partial t} + \psi_y\frac{\partial}{\partial x} + \delta\psi_x\frac{\partial}{\partial y})\theta = \frac{1}{\mathrm{Pr}}(c^2\delta^2\frac{\partial^2}{\partial t^2} + \delta^2\frac{\partial^2}{\partial x^2} + \frac{\partial^2}{\partial y^2})\theta + Ec[(\frac{\partial \psi_y}{\partial y} + \delta^2\frac{\partial \psi_x}{\partial x})^2 + 2\delta^2(\frac{\partial^2\psi_y}{\partial x^2})^2$$
$$+ 2\delta(\frac{\partial^2\psi_x}{\partial y^2})] \tag{3.10}$$

where

$$\tau_{xx} = -2[1+n(We\dot{\gamma}-1)]\frac{\partial u}{\partial x},\ \ \tau_{xy} = -[1+n(We\dot{\gamma}-1)](\frac{\partial u}{\partial y}+\delta^2\frac{\partial v}{\partial x}),\ \ \tau_{yy} = -2\delta[1+n(We\dot{\gamma}-1)]\frac{\partial v}{\partial y}$$

The stream function (ψ) is connected with the velocity components by the relations

$$U = \frac{\partial \psi}{\partial y}, \qquad V = -\delta\frac{\partial \psi}{\partial x}$$

the non-dimensional variables defined in Eqs.(11) (12),(13) gives the following equation

$$Re\delta\left(\psi_y\frac{\partial}{\partial x} - \psi_x\frac{\partial}{\partial y}\right)\psi_y = -\frac{\partial p}{\partial x} + \delta\frac{\partial S_{xx}}{\partial x} + \frac{\partial S_{xy}}{\partial y} - Ha^2\cos\beta^*((\psi_y+1)cos\beta^* + \delta\psi_x\sin\beta^*) - \frac{1}{\mathrm{Da}}\psi_y \tag{3.11}$$

$$Re\delta^3\left(\psi_y\frac{\partial}{\partial x} - \psi_x\frac{\partial}{\partial y}\right)\psi_x = -\frac{\partial p}{\partial y} + \delta^2\frac{\partial S_{xy}}{\partial x} + \delta\frac{\partial Syy}{\partial y} + \delta Ha^2\sin\beta^*\left((\psi_y+1)cos\beta^* + \delta\psi_x\sin\beta^*\right) - \frac{\delta}{\mathrm{Da}}\psi_x \tag{3.12}$$

Elimination of p between Eqs.(3.11) and (3.12) yields

$$Re\delta\left(\psi_y\frac{\partial}{\partial x} - \psi_x\frac{\partial}{\partial y}\right)\nabla^2\psi = \delta\left[\frac{\partial^2}{\partial x\partial y}(\tau_{xx}-\tau_{yy})\right] + \left[\frac{\partial^2}{\partial y^2} - \delta^2\frac{\partial^2}{\partial x^2}\right]S_{xy} - Ha^2\cos^2\beta^*\left(\frac{\partial^2\psi}{\partial y^2} - \right.$$
$$\left.\delta^2 Ha^2\sin^2\beta^*\frac{\partial^2\psi}{\partial x^2}\right) - \delta\ Ha^2\cos\ \beta^*\sin\beta^*\psi_{xy}\ - \frac{1}{\mathrm{Da}}(\psi_{yy} - \delta\psi_{xy}) \tag{3.13}$$

where

$$\nabla^2 = \delta^2 \frac{\partial^2}{\partial x^2} + \frac{\partial^2}{\partial y^2}$$

The dimensionless boundary conditions in the wave frame are

$$\psi = \frac{F}{2}, \quad \frac{\partial \psi}{\partial y} = -1 \qquad at \quad y = h_1. \tag{3.14}$$

$$\psi = \frac{-F}{2}, \quad \frac{\partial \psi}{\partial y} = -1 \qquad at \quad y = h_2 \tag{3.15}$$

$$\theta = 0 \qquad at \quad y = h_1, \qquad \theta = 1 \quad at \qquad y = h_2 \tag{3.16}$$

where F is the dimensionless time mean flow rate in the wave frame. It is related to the dimensionless time mean flow rate Q_1 in the laboratory frame through the expression

$$Q_1 = F + 1 + d. \tag{3.17}$$

The dimensionless forms of $h_1(x)$ and $h_2(x)$ are

$$h_1(x) = 1 + a \sin x, \qquad h_2(x) = -d - b \sin(x + \phi) \tag{3.18}$$

where a, b, ϕ and d satisfy:

$$a^2 + b^2 + 2ab \cos \phi \leq (1 + d)^2.$$

4. Solution of the problem

The Eq.(3.13) is highly non-linear and complicated; therefore it is impossible to obtain closed form solution for all the involving arbitrary parameters . So we employ the perturbation technique to find the solution. For perturbation solution, we expand.

$$\begin{aligned} \psi &= \psi_0 + We\psi_1 + o(We^2) \\ F &= F_0 + We\ F_1 + o(We^2) \\ p &= p_0 + We\ p_1 + o(We^2) \end{aligned} \tag{4.1}$$

and substitute the expressions (3.16) into Eqs. (3.9)-(3.11) with boundary conditions Eq.(3.12) and Eq.(3.13), equating the coefficients of like powers of We, we get the following system of equations:

4.1. Zero order system

In the zeroth order system , negligible the terms of order We, we get

$$\frac{\partial^2 \tau_{0xy}}{\partial y^2} - m\psi_{0yy} = 0 \tag{4.2}$$

$$m = \frac{\sqrt{Ha^2 \cos^2 \beta - \frac{1}{Da} + \sigma^2}}{n - 1} \tag{4.3}$$

From Eq. (3.9) we get

$$\frac{\partial p_0}{\partial x} = \frac{\partial}{\partial y} \tau_{0xy} - m(\psi_y + 1) \tag{4.4}$$

And from Eq.(3.10) we get

$$\frac{\partial p}{\partial y} = 0 \tag{4.5}$$

Such

$$\tau_{0xy} = \psi_{0yy}^2 \tag{4.6}$$

$$\psi_0 = \frac{F_0}{2}, \quad \frac{\partial \psi_0}{\partial y} = -1 \;\; at \;\; y = h_1 \; and \quad \psi_0 = -\frac{F_0}{2}, \quad \frac{\partial \psi_0}{\partial y} = -1 \;\; at \;\; y = h_2 \tag{4.7}$$

4.2. First order system

$$\frac{\partial^2 \tau_{1xy}}{\partial y^2} + (\frac{n}{n-1})\frac{\partial^2}{\partial y^2}[(\psi_{0yy})^2] - m\psi_{1yy} = 0 \tag{4.8}$$

$$\frac{\partial p_1}{\partial x} = \frac{\partial^3 \psi 1}{\partial y^3} + (\frac{n}{n-1})\frac{\partial}{\partial y}[(\psi_{0yy})^2] - m\psi_{1y} = 0 \tag{4.9}$$

$$\psi_1 = \frac{F_1}{2}, \quad \frac{\partial \psi_1}{\partial y} = -1 \;\; at \;\; y = h_1 \;\; and \;\; \psi_1 = -\frac{F_1}{2}, \quad \frac{\partial \psi_1}{\partial y} = -1 \;\; at \;\; y = h_2 \tag{4.10}$$

In solving the corresponding zeroth and first order system we obtain the final expression for stream function

$$\psi = \frac{e^{-\sqrt{m}y}(e^{2\sqrt{m}y}c_1 + c_2)}{m} + c3y + c4 + We\left(\frac{\frac{e^{2(h_1+h_2)\sqrt{m}(h_1-h_2)^2(1+m)^2m^2n}}{\xi}}{3m}\right)A3 + A4y \tag{4.11}$$

$$\xi = e^{h_2\sqrt{m}}\left(-2 + h_1(-1+m)\sqrt{m} - h_2(-1+m)\sqrt{m}\right) + e^{h_1\sqrt{m}}\left(2 + h_1(-1+m)\sqrt{m}\right)^2(-1+m) \tag{4.12}$$

In solving the corresponding zeroth and first order system we obtain the final expression for stream function

$$u = \psi_{0y} + We\psi_{1y} \tag{4.13}$$

4.3. Solution of energy equation

Applying the long wavelength and low Reynolds number approximation on Eq.(3.10), we get

$$0 = \frac{1}{\mathrm{Pr}}\left(\frac{\partial^2}{\partial y^2}\right)\theta + Ec\left(\frac{\partial^2 \psi}{\partial y^2}\right)^2 \tag{4.14}$$

The solution of Eq. (4.14) with boundary conditions Eq. (3.16) can be written as
$\theta = c_1 + c_2y + y_2Ec(h_1 - h_2)2(-1+m)2mnprWe)(12e_2h_1m + 2my - 24eh_1m + h_2m + 2my + 12e_2h_2m + 2my - 12e_2h_1m + 2myh_1m + 12e_2h_2m + 2myh_1m + 12e_2h_1m + 2myh_2m - 12e_2h_2m + 2myh_2m + 3e_2h_1m + 2myh_12m + 6eh_1m + h_2m + 2myh_{12}m + 3e_2h_2m + 2myh_{12}m - 6e_2h_1m + 2myh_1h_2m - 12eh_1m + h_2m + 2myh_1h_2m - 6e_2h_2m + 2myh_1h_2m + 3e_2h_1m + 2myh_{22}m + 6eh_1m + h_2m + 2myh_{22}m + 3e_2h_2m + 2myh_2 2m + 12e_2h_1m + 2myh_1m_{32} - 12e_2h_2m + 2myh_1m_{32} - 12e_2h_1m + 2myh_2m_{32} + 12e_2h_2m + 2myh_2m_{32} - 6e_2h_1m + 2myh_{12}m_2 - 12eh_1m + h_2m + 2myh_{12}m_2 - 6e_2h_2m + 2myh_{12}m_2 + 12e_2h_1m +$

$2myh_1h_2m_2+24eh_1m+h_2m+2myh_1h_2m_2+12e_2h_2m+2myh_1h_2m_2-6e_2h_1m+2myh_{22}m_2-12eh_1m+h_2m+2myh_{22}m_2-6e_2h_2m+2myh_{22}m_2+3e_2h_1m+2myh_{12}m_3+6eh_1m+h_2m+2myh_{12}m_3+3e_2h_2m+2myh_{12}m_3-6e_2h_1m+2myh_1h_2m_3-12eh_1m+h_2m+2myh_1h_2m_3-6e_2h_2m+2myh_1h_2m_3+3e_2h_1m+2myh_{22}m_3+6eh_1m+h_2m+2myh_{22}m_3+3e_2h_2m+2myh_{22}m_3-12e_2h_1m+2myn+24eh_1m+h_2m+2myn-12e_2h_2m+2myn+12e_2h_1m+2myh_1mn-12e_2h_2m+2myh_1mn-12e_2h_1m+2myh_2mn+12e_2h_2m+2myh_2mnpr,$
c_1 and c_2 are constant can be determined from the boundary conditions.

5. Results and discussion

This section is divided in to sub sections. In the first, the temperature field distribution is discussed. In the second, the flow characteristics are illustrated using the software MATHEMATICA. These resulte are in good agreement with those reported by [5].

5.1. The temperature field distribution

Many parameters are effected by the temperature field such as Prandtl number (Pr) , Eckert number (Ec), Hartman number (Ha), Weissnberg number (We), Darcy number (Da), phase different (ϕ), inclined parameter B and law number (n) from Figures (4) ,(5), (6) and (9) show that the increasing in each of Hartman number (Ha), Weissnberg number (We), Darcy number (Da) and law number (n) leads to decreasing in the temperature. While the increasing in Prandtl number (Pr) , Eckert number (Ec) leads to increasing in the temperature, see Figures, (2) and (3) Figure.(7) and (8) show that there is a very small change in temperature with increasing phase different and inclined parameter B.

5.2. Pumping characteristic

Figs 10-17 portray the variety of pressure rise in capacity of volumetric stream rate in the wave outline for various estimations of the Hartmann number (Ha) , inclined magnetic parameter (β) ,Weissbering number (We), law number (n) , Darcy number (Da) and phase different (ϕ). The whole region is considered into five parts (i) peristaltic pumping region where $(\nabla p > 0, \quad F > 0)$. (ii) augmented pumping(co- pumping) region where $(\nabla p < 0, \quad F > 0)$. (iii) when $(\nabla p > 0, \quad F < 0)$. Then it is a retrograde pumping region. (iv) There is a co-pumping region where $(\nabla p < 0, \quad F < 0)$. (v) $(\nabla p = 0)$ corresponds to the free pumping region. Figure. 11, shows that pressure rise increases with increasing Hartmann number Ha. It can be seen from the graph that in a retrograde region It can be seen from the graph that in a retrograde region $(\nabla p > 0, \quad F < 0)$, the pumping rate decreases in a co¬pumping region where $(\nabla p < 0, \quad F > 0)$. with an increase in Ha. Figure. 10, shows that pressure rise p decreases with increasing Weissbering number (We). It is observed that the pumping rate increases in the co¬pumping region $(\nabla p < 0$, and free pumping region $(\nabla p = 0$.. Figure.12 shows that pressure rise p decreases with increasing inclined parameter B. It is observed that in a retrograde pumping region $(\nabla p > 0, \quad F < 0)$., the pumping rate increases a co-pumping region where $(\nabla p < 0$, with an increase in B. Fig.13 shows that pressure rise ∇p decreases with increasing law number (n). It is observed that in a retrograde pumping region $(\nabla p > 0, \quad F < 0)$.,the pumping rate increases in a co-pumping region where $(\nabla p < 0$ with an increase in (n). From Fig.14 shows that pressure rise ∇p increases with increasing Darcy number (Da). It can be seen from the graph that in a retrograde region $(\nabla p > 0, \quad F > 0)$., the pumping rate decreases in a co¬pumping region where $(\nabla p > 0, \quad F < 0)$. with an increase in (Da). Fig.15 shows that pressure rise p decreases with increasing phase different (ϕ).It is observed the pumping increases in the region of augmented pumping and the co¬pumping region $(\nabla p < 0$.

5.3. Velocity distribution

Figures. 16-21 represent the variation of axial velocity u across the channel for different values of the Hartmann number (Ha), the Darcy number (Da), the inclined parameter (B), law number (n), Weissberng number (We) and phase difference

Figure. 16 shows that the axial velosity decreases in the central region of the channel with increasing Hartmann number Ha, while the axial velocity increases in the boundary of the channel wall. The reason behind this fact is the Lorentz force that arises due to the application of an inclined magnetic feild , which plays a vital role in decelerating the fluid motion. Similarly the axial velocity has reducing effect at the central region of the channel and accelerating effect near the the channel wall for increasing Darcy number (Da) as shown in Figure 17. In this case velocity decreases due to the increase of particle size suspended in the fluid itself and causes flattening of the velocity profiles. In order to satisfy the conservation of mass, the flow rate remains same for any value of these parameters at any cross section of the channel. From Figure. 21 shows that the axial velocity decreases in the central region of the channel with increasing the phase difference parameter while the axial velocity increases near the the channel wall.

From Figure.19, we observed that the axial velocity also decreases at the central region with increasing the law number (n) of the channel, while the axial velocity increases in the boundary of the channel wall. It is examined. Figure. 20, we observed that the axial velocity increase at the central region with the increase of the Weissberng number (We), while the axial velocity decreases in the boundary of the channel wall.

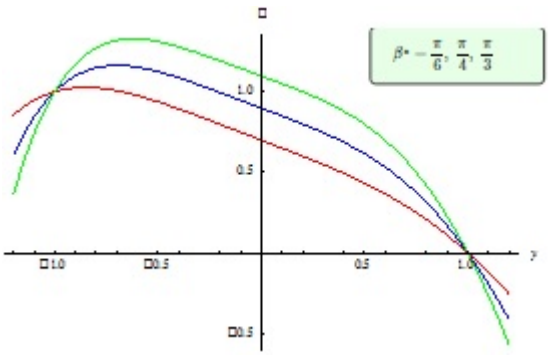

Figure 2: The variation of temperature with y for different value of Ec at $n = 1.5$, $Pr = 1$, $Q_1 = 1.1$, $Ha = 1$, $\phi = 0.5$, $a = 0.2$, $b = 0.2$, $d = 0.5$, $We = 1.5$, $Da = 0.2$.

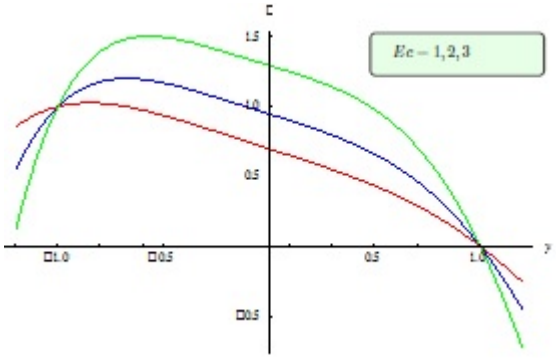

Figure 3: The variation of temperature with y for different value of Ec at $n = 1.5$, $Pr = 1$, $Q_1 = 1.1$, $Ha = 1$, $\phi = 0.5$, $a = 0.2$, $b = 0.2$, $d = 0.5$, $We = 1.5$, $Da = 0.2$.

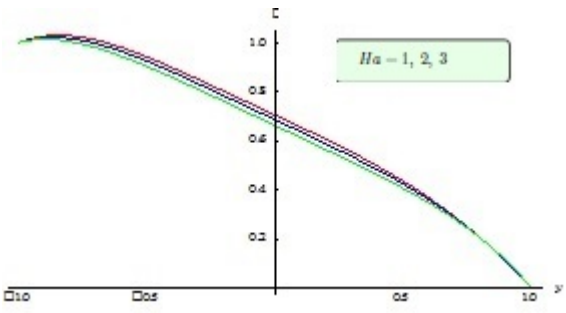

Figure 4: The variation of temperature with y for different value of Ec at $n = 1.5$, $Pr = 1$, $Q_1 = 1.1$, $Ha = 1$, $\phi = 0.5$, $a = 0.2$, $b = 0.2$, $d = 0.5$, $We = 1.5$, $Da = 0.2$.

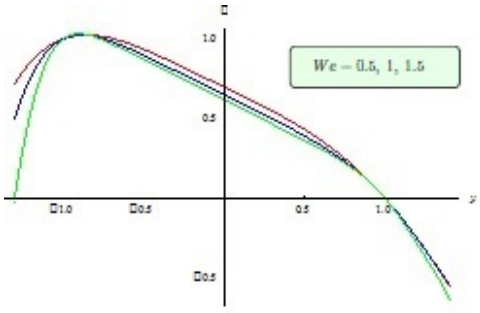

Figure 5: The variation of temperature with y for different value of Ec at $n = 1.5$, $Pr = 1$, $Q_1 = 1.1$, $Ha = 1$, $\phi = 0.5$, $a = 0.2$, $b = 0.2$, $d = 0.5$, $We = 1.5$, $Da = 0.2$.

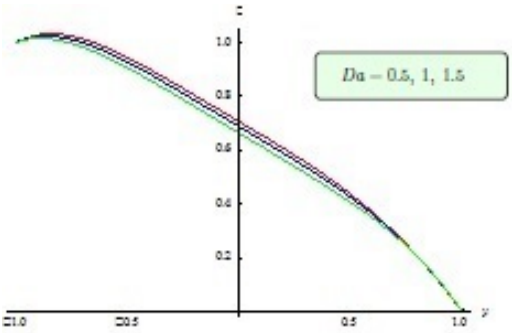

Figure 6: The variation of temperature with y for different value of Ec at $n = 1.5$, $Pr = 1$, $Q_1 = 1.1$, $Ha = 1$, $\phi = 0.5$, $a = 0.2$, $b = 0.2$, $d = 0.5$, $We = 1.5$, $Da = 0.2$.

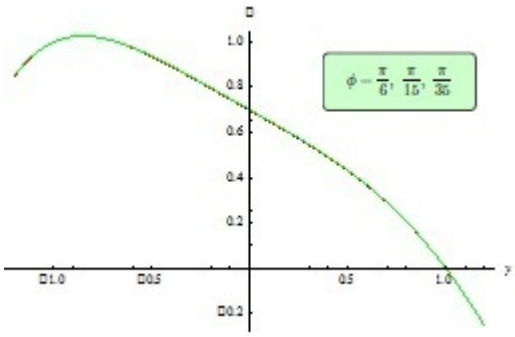

Figure 7: The variation of temperature with y for different value of Ec at $n = 1.5$, $Pr = 1$, $Q_1 = 1.1$, $Ha = 1$, $\phi = 0.5$, $a = 0.2$, $b = 0.2$, $d = 0.5$, $We = 1.5$, $Da = 0.2$.

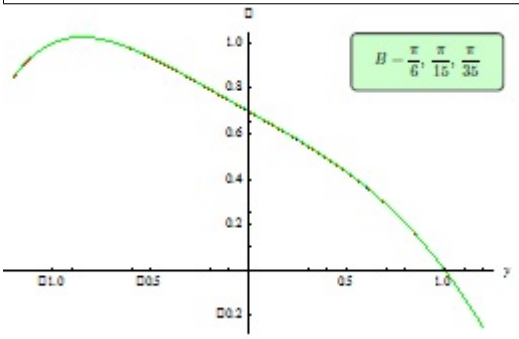

Figure 8: The variation of temperature with y for different value of Ec at $n = 1.5$, $Pr = 1$, $Q_1 = 1.1$, $Ha = 1$, $\phi = 0.5$, $a = 0.2$, $b = 0.2$, $d = 0.5$, $We = 1.5$, $Da = 0.2$.

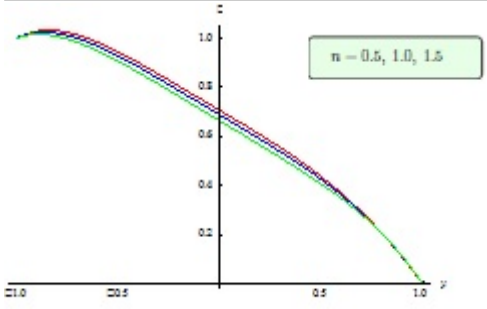

Figure 9: The variation of temperature with y for different value of Ec at $n = 1.5$, $Pr = 1$, $Q_1 = 1.1$, $Ha = 1$, $\phi = 0.5$, $a = 0.2$, $b = 0.2$, $d = 0.5$, $We = 1.5$, $Da = 0.2$.

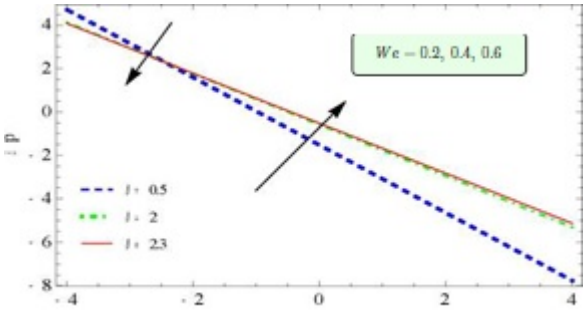

Figure 10: The variation of temperature with y for different value of Ec at $n = 1.5$, $Pr = 1$, $Q_1 = 1.1$, $Ha = 1$, $\phi = 0.5$, $a = 0.2$, $b = 0.2$, $d = 0.5$, $We = 1.5$, $Da = 0.2$.

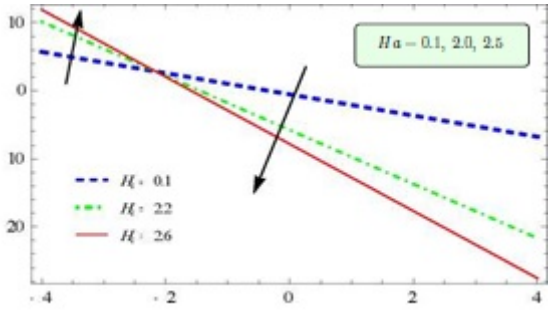

Figure 11: The variation of temperature with y for different value of Ec at $n = 1.5$, $Pr = 1$, $Q_1 = 1.1$, $Ha = 1$, $\phi = 0.5$, $a = 0.2$, $b = 0.2$, $d = 0.5$, $We = 1.5$, $Da = 0.2$.

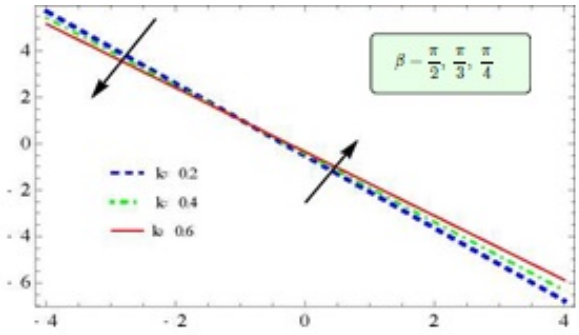

Figure 12: The variation of temperature with y for different value of Ec at $n = 1.5$, $Pr = 1$, $Q_1 = 1.1$, $Ha = 1$, $\phi = 0.5$, $a = 0.2$, $b = 0.2$, $d = 0.5$, $We = 1.5$, $Da = 0.2$.

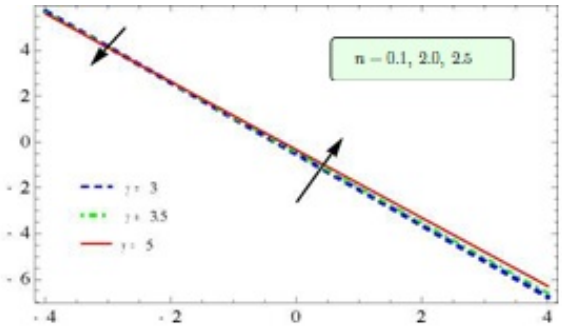

Figure 13: The variation of temperature with y for different value of Ec at $n = 1.5$, $Pr = 1$, $Q_1 = 1.1$, $Ha = 1$, $\phi = 0.5$, $a = 0.2$, $b = 0.2$, $d = 0.5$, $We = 1.5$, $Da = 0.2$.

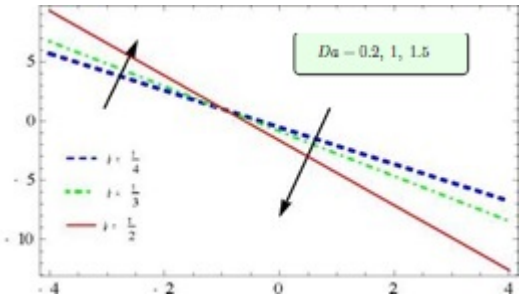

Figure 14: The variation of temperature with y for different value of Ec at $n = 1.5$, $Pr = 1$, $Q_1 = 1.1$, $Ha = 1$, $\phi = 0.5$, $a = 0.2$, $b = 0.2$, $d = 0.5$, $We = 1.5$, $Da = 0.2$.

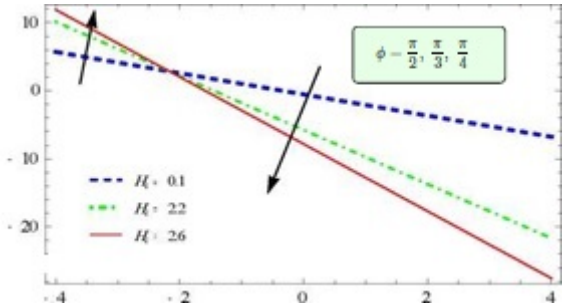

Figure 15: The variation of temperature with y for different value of Ec at $n = 1.5$, $Pr = 1$, $Q_1 = 1.1$, $Ha = 1$, $\phi = 0.5$, $a = 0.2$, $b = 0.2$, $d = 0.5$, $We = 1.5$, $Da = 0.2$.

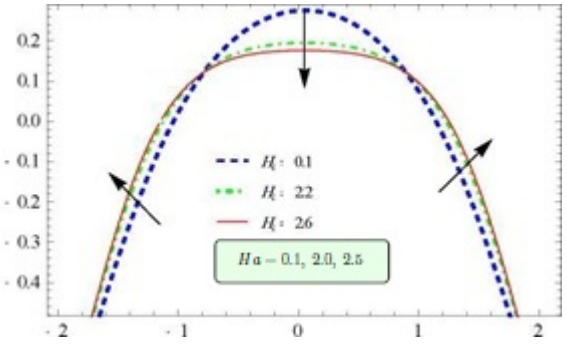

Figure 16: The variation of temperature with y for different value of Ec at $n = 1.5$, $Pr = 1$, $Q_1 = 1.1$, $Ha = 1$, $\phi = 0.5$, $a = 0.2$, $b = 0.2$, $d = 0.5$, $We = 1.5$, $Da = 0.2$.

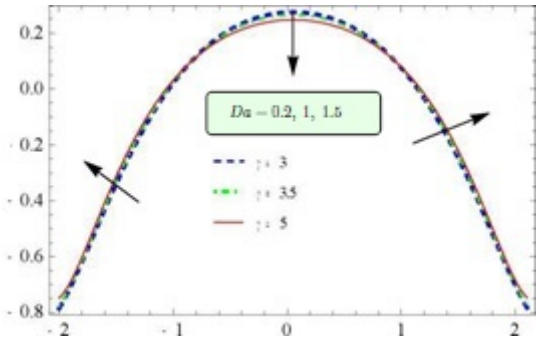

Figure 17: The variation of temperature with y for different value of Ec at $n = 1.5$, $Pr = 1$, $Q_1 = 1.1$, $Ha = 1$, $\phi = 0.5$, $a = 0.2$, $b = 0.2$, $d = 0.5$, $We = 1.5$, $Da = 0.2$.

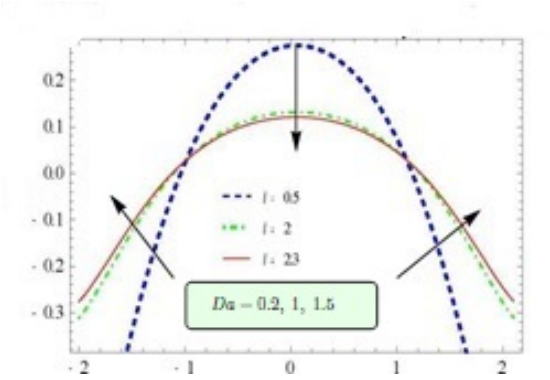

Figure 18: The variation of temperature with y for different value of Ec at $n = 1.5$, $Pr = 1$, $Q_1 = 1.1$, $Ha = 1$, $\phi = 0.5$, $a = 0.2$, $b = 0.2$, $d = 0.5$, $We = 1.5$, $Da = 0.2$.

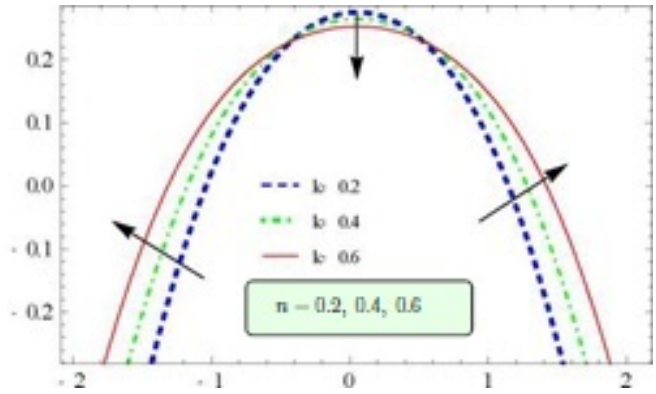

Figure 19: The variation of temperature with y for different value of Ec at $n = 1.5$, $Pr = 1$, $Q_1 = 1.1$, $Ha = 1$, $\phi = 0.5$, $a = 0.2$, $b = 0.2$, $d = 0.5$, $We = 1.5$, $Da = 0.2$.

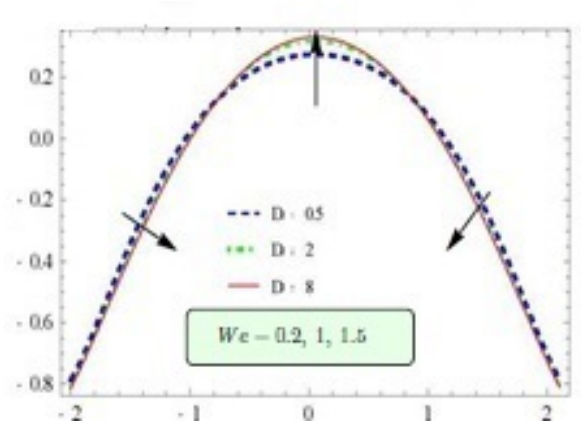

Figure 20: The variation of temperature with y for different value of Ec at $n = 1.5$, $Pr = 1$, $Q_1 = 1.1$, $Ha = 1$, $\phi = 0.5$, $a = 0.2$, $b = 0.2$, $d = 0.5$, $We = 1.5$, $Da = 0.2$.

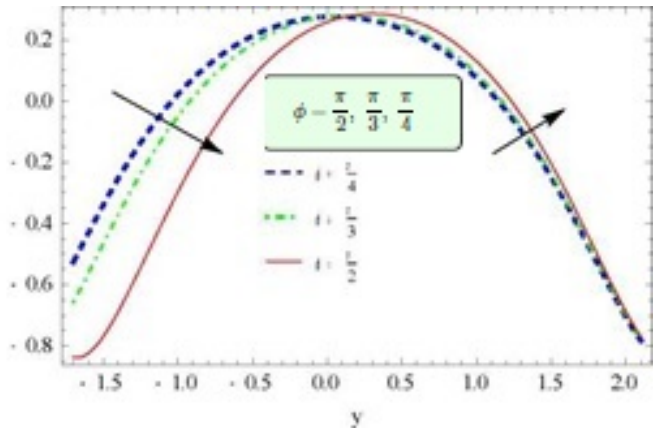

Figure 21: The variation of temperature with y for different value of Ec at $n = 1.5$, $Pr = 1$, $Q_1 = 1.1$, $Ha = 1$, $\phi = 0.5$, $a = 0.2$, $b = 0.2$, $d = 0.5$, $We = 1.5$, $Da = 0.2$.

6. Conclusions

In this paper, we have theoretically studied the effect .heat transfer with the activity of connected inclined magnetic felid of asymmetric channel through the .porous medium . In this investigation, special emphasis has been paid to study such as velocity distribution, the pumping characteristic and heat transfer on the basis of a simple analytical solution.

- The axial velocity at the central region decreases with the increasing values of the Hartmann number (Ha), Darcy number (Da), the inclined parameter (B) and power law number (n), whereas it increases in the boundary of the channel wall.
- The axial at the central region increases with the increasing values of Weissberng number (We), whereas it decreases in the boundary of the channel wall.
- There is a linear relationship between pressure rise for each wave length and volumetric flow rate.
- The pressure rise increases in retrograde pumping with the increasing value (B) , (We) and (n) whereas it decreases with the increasing values, $(Da), (Ha), (k)$ and (ϕ).
- The temperature transfer decreases with the increasing values of the (Ha), (Da), (n) and (We), whereas it increases with increasing (Ec) and (Pr).

References

[1] A.D. Ajaz and K. Elangovan, *Influence of an inclined magnetic field and rotation on the peristaltic flow of a micropolar fluid in an inclined channel*, New J. Sci. 14 (2016).

[2] H. Branover, *Magneto hydrodynamics Flow in Ducts*, Wiley, NewYork, 1978.

[3] T. Hayat, F.M. Mahomed and S. Asghar, *Peristaltic flow of amagnetohydrodynamic Johnson-Segalman fluid*, Nonlinear Dyn. 40 (2005) 375–85.

[4] T. Hayat, M. Khan and S. Asghar, *Peristaltic transport of a third order fluid under the effect of a magnetic field*, 53 (2006) 1074–1087

[5] S. Jyothi, M. V. Subba Reddy and P. Gangavathi, *Hyperbolic tangent fluid flow through a porous medium in an inclined Cjhannel with peristalsis*, Int. J. Adv. Sci. Res. Manag. 1 (2016) 2455–6378.

[6] M.R. Krishnamurthy, B.C. Prasannakumara, B.J. Gireesha, R.S.R. Gorla, *Effect of viscous dissipation on hydromagnetic fluid flow and heat transfer of nanofluid over an exponentially stretching sheet with fluid-particle suspension*, Cogent. Math. 2 (2015) 1–19.

[7] S. Mansur, A. Ishak and I. Pop, *Flow and heat transfer of nanofluid past shrinking/stretching sheet with partial slip boundary conditions*, Appl. Math. Mech. 35 (2014) 1401–1410.

[8] OU. Mehmood and T. Hayat, *Slip effect on MHD flow of third order fluid in a planar channel*, Commun. Nonlinear Sci. Numer. Simulat. 16 (2011) 1363-1377.

[9] Kh. S Mekheimer, *Effect of the induced magnetic field on peristaltic flow of a couple stress fluid*, Phys. Lett. A 372 (2008) 4271.

[10] G. Nagachandrakala, A. leelarathnam and S. Sreenadh, *Influence of slipconditions on MHD peristaltic flow of a hyperbolic tangent fluid in a non-uniform porous channel with wall properties*, Int. Engin. Sci. Tech. 5 (2013).

[11] N. Sandeep and V. Sugunamma, *Radiation and IMF effects on unsteady hydromagnetic free convection flow past an impulsively moving vertical plate in a PM*, J. Appl. Math. Fluid Mech. 7 (2014) 275–286.